Engineering xxx (xxxx) xxx

Contents lists available at ScienceDirect

Engineering

journal homepage: www.elsevier.com/locate/eng

Research
Watershed Ecology—Article

Dynamic Modeling Framework of Sediment Trapped by Check-Dam Networks: A Case Study of a Typical Watershed on the Chinese Loess Plateau

Pengcheng Sun [a,b,c], Yiping Wu [a,c,*]

[a] Key Laboratory of Degraded and Unused Land Consolidation Engineering, Shaanxi Land Engineering Construction Group Co. Ltd., Xi'an 710075, China
[b] Key Laboratory of Soil and Water Conservation on the Loess Plateau of Ministry of Water Resources, Yellow River Institute of Hydraulic Research, Zhengzhou 450003, China
[c] Technology Innovation Center for Land Engineering and Human Settlements, Shaanxi Land Engineering Construction Group Co. Ltd. & Xi'an Jiaotong University, Xi'an 710115, China

ARTICLE INFO

Article history:
Received 24 February 2021
Revised 24 April 2021
Accepted 17 December 2021
Available online 25 February 2022

Keywords:
Check dams
Dynamic check dam (DCDam)
Loess Plateau
Sediment trapping
SWAT

ABSTRACT

Check-dam construction is an effective and widely used method for sediment trapping in the Yellow River Basin and other places over the world that are prone to severe soil erosion. Quantitative estimations of the dynamic sediment trapped by check dams are necessary for evaluating the effects of check dams and planning the construction of new ones. In this study, we propose a new framework, named soil and water assessment tool-dynamic check dam (SWAT-DCDam), for modeling the sediment trapped by check dams dynamically, by integrating the widely utilized SWAT model and a newly developed module called DCDam. We then applied this framework to a typical Loess watershed, the Yan River Basin, to assess the time-varying effects of check dam networks over the past 60 years (1957–2016). The DCDam module generated a specific check dam network to conceptualize the complex connections at each time step (monthly). In addition, the streamflow and sediment load simulated by using the SWAT model were employed to force the sediment routing in the check dam network. The evaluation results revealed that the SWAT-DCDam framework performed satisfactorily, with an overestimation of 11.5%, in simulating sediment trapped by check dams, when compared with a field survey of the accumulated sediment deposition. For the Yan River Basin, our results indicated that the designed structural parameters of check dams have evolved over the past 60 years, with higher dams (37.14% and 9.22% increase for large dams and medium dams, respectively) but smaller controlled areas (46.03% and 10.56% decrease for large dams and medium dams, respectively) in recent years. Sediment retained by check dams contributed to approximately 15.0% of the total sediment load reduction in the Yan River during 1970–2016. Thus, our developed framework can be a promising tool for evaluating check-dam effects, and this study can provide valuable information and support to decision-making for soil and water conservation and check-dam planning and management.

1. Introduction

Soil erosion is recognized as a severe global hazard. Extreme soil erosion is linked to several natural environmental and socio-economic challenges worldwide(e.g., food shortage, water crisis, and biodiversity loss), owing to both on-site (e.g., land degradation, loss of fertility, and damage to biotas) and off-site (e.g., sedimentation, siltation, and eutrophication of water ways and enhanced floods) effects [1,2], threatening the realization of multiple targets in the Sustainable Development Goals (SDGs), such as land degradation neutrality (SDG15.3) and water-related ecosystem protection (SDG6.6) [3–5]. Several types of restoration strategies and control measures have been implemented worldwide to control soil erosion, including measures implemented on slopes (e.g., afforestation, conservation tillage, and terraces) and measures applied in channels (e.g., check dams, bed sills, and bank protection structures).

Among all the soil conservation measures, check dams constructed along gullies and channels are one of the most effective and widely used methods for trapping sediment and alleviating soil erosion [6]. They are usually defined as transverse structures

* Corresponding author.
E-mail address: yipingwu@xjtu.edu.cn (Y. Wu).

https://doi.org/10.1016/j.eng.2021.12.015

Please cite this article as: P. Sun and Y. Wu, Dynamic Modeling Framework of Sediment Trapped by Check-Dam Networks: A Case Study of a Typical Watershed on the Chinese Loess Plateau, Engineering, https://doi.org/10.1016/j.eng.2021.12.015

built across stream beds to control water flow and sediment transfer [7,8]. These permanent or temporary channel structures were built using various materials, such as stones, earths, wood logs, and straw bales, and their construction history can be traced back to approximately 100 years [7,9,10]. Numerous check dams have been constructed worldwide, especially in erosion-prone regions with high-density gullies, such as China, Spain, the United States, Italy, and Ethiopia [6]. Approximately 269 check dams were reported to have been built in an area of 2.39 km^2 in southwestern Spain [11]. In China, more than 58 000 check dams had been constructed on the Loess Plateau by the end of 2011, among which 5655 large check dams had been built with a total storage of more than 5.70×10^9 m^3 [12]. High-density check dams have been constructed along channels and linked with streams in multiple connections, forming complex check dam networks. These check dams and dam networks have played an important role in watershed management with multiple functions, such as alleviating soil loss and controlling sediment yield from watersheds [13,14], reducing flood peak and storing water for irrigation and groundwater recharge [15,16], controlling riverbed scouring and consolidating slopes [8,17], trapping sediment and the attached nutrients for cultivation [18,19], and providing scientific information for understanding the hydrological and erosional systems [20,21].

The evaluation of long-term sediment trapping and deposition by check dams is important for estimating sediment yield, inferring soil erosion and sediment sources [22,23], and examining the trapping effectiveness [24]. Moreover, the regional estimation of sediment trapped by check dams is critical for assessing the effects of check dams on river sediment load reduction [25] and evaluating the available storage to support the planning of new check dams. Various methods have been developed to estimate the amount of sediment trapped by check dams in recent decades, including field-work-based methods (the section and topographic methods) and the modeling method based on numerical simulations. Field-work-based methods are usually used to calculate the amount of sediment based on the estimated deposition volume through field surveys [26], and it can be applied to only a limited number of check dams because it is time-consuming and costly. For example, the volume of sediment deposition is estimated based on the trench profiles, boreholes, or drillings when the section method is used [27,28], considerably limiting its application to a large number of check dams. Geometric and topographic methods can be employed at a regional scale [11], especially when combined with unmanned aerial systems; however, they only provide the accumulated sediment deposition instead of the dynamic deposition history. Numerical models can be a promising alternative for simulating sediment yield from upper streams and estimating the amount of sediment trapped by check dams. For example, Li et al. [29] estimated the sediment trapped by 20 separate check dams using the reservoir module in the Soil and Water Assessment Tools (SWAT), without considering the check-dam network and connections between dams. Pal et al. [30] proposed a numerical framework based on the Sediment Delivery Model, to simulate sediment deposition in check dams at the annual scale, but did not consider the temporal changes in check dam networks caused by the construction of new dams.

Although some progress has been made in the estimation of sediment deposition by check dams using different field observations or modeling methods, only a few studies have been conducted to describe the dynamic sediment deposition in a changing check-dam network, including the changes in the available storage and network structure. In addition, in a few studies, the check-dam operation and tightly associated hydrological and sediment transport in watershed modeling and/or management have been integrated. Therefore, the specific objectives of this study were to ① establish a method to automatically generate a temporally changing check dam network, ② develop a new module for describing the sediment routing in a check dam network, and ③ integrate the newly developed module with the hydrological model, SWAT, to formulate a framework for simulating watershed hydrological processes and accompanying sediment transport and dynamic sediment trapping by check-dam networks, by conducting a case study of a typical watershed on the Chinese Loess Plateau.

2. Materials and methods

2.1. Study area

We selected the Yan River Basin (YanRB) as the typical study area, with the study period being from 1957 to 2016. The YanRB is located at the center of the Chinese Loess Plateau (Fig. 1), covering an area of 7725 km^2, with an elevation ranging from 480 to 1790 m (Fig. 1). It originates from the Zhou mountain in the northern Shannxi province, flows from the northwest to the southeast, and discharges into the Yellow River, with a mainstream of 286.9 km. The YanRB is characterized by a temperate continental semiarid climate with a mean temperature of 9.0 °C. The average annual rainfall during the 60-year study period (1957–2016) was 516 mm, with more than 70% of the annual precipitation occurring during the wet season (June to September). The YanRB is covered by thick loess, which is an erosion-prone silty-loam soil. There are three major land use types: grassland, cropland, and forestland, and they accounted for 62.36%, 33.53%, and 4.02% of the total land area, respectively, in 1975. Large-scale ecological restoration measures have been implemented in the YanRB to alleviate severe soil erosion and reduce its high sediment load to the Yellow River since the late 1960s and early 1970s [31,32]. The forestland in the YanRB increased from 4.02% in 1975 to 26.20% in 2010, whereas the cropland decreased from 33.53% to 17.60%. Moreover, more than 800 check dams had been constructed by the end of 2008 (Fig. 2), and the check-dam construction in this basin was rated as featured projects by the Ministry of Water Resources of China in 2003 [33].

2.2. SWAT model

The SWAT model, a temporally continuous, physically based, and hydrologically distributed model, was developed by the Agricultural Research Services of the US Department of Agriculture [34,35]. The model has been widely utilized to investigate the effects of land use management and climate change on water, sediment, and nutrient yields at the watershed scale [36–38]. The SWAT model was employed to divide the basin into sub-basins connected with streams and further delineate the hydrological response units (HRUs) within each sub-basin, considering the combinations of land use, soil, and slopes. Water, sediment, and nutrients computed from each HRU were routed to the outlet of the corresponding sub-basin. SWAT provided most of the hydrological components as model outputs, mainly including surface runoff, lateral flow, baseflow, evapotranspiration, soil water content, water yield, sediment load, and nutrient loads. Details on the mechanisms of SWAT can be found in the theoretical documentation [35], and details about the input and output files of the model can be found in the input/output documentation [39].

2.3. Data collection

Daily meteorological data, namely, precipitation, maximum and minimum temperature, relative humidity, wind speed, and sunshine duration, for five weather stations were collected from the Data Center of the China Meteorological Administration[†]. Solar

[†] http://data.cma.cn

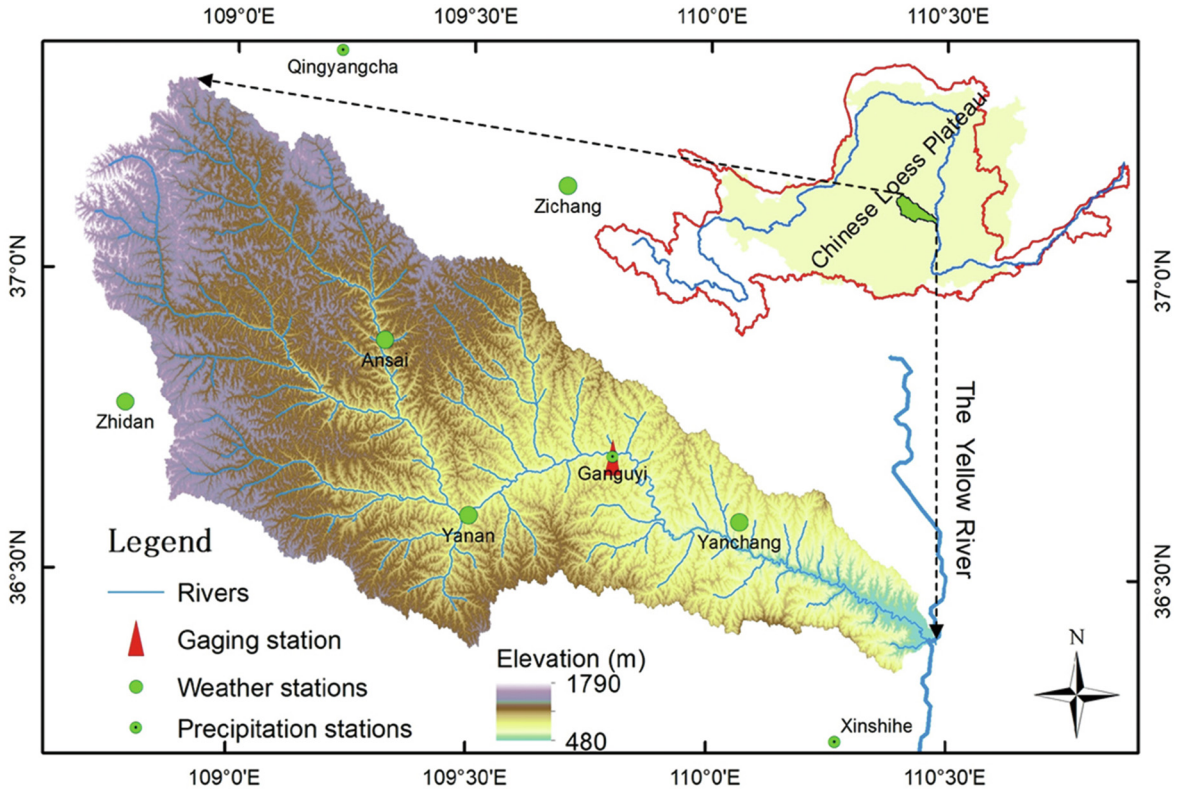

Fig. 1. Location of the Yan River Basin (YanRB) and the monitoring stations used in the study.

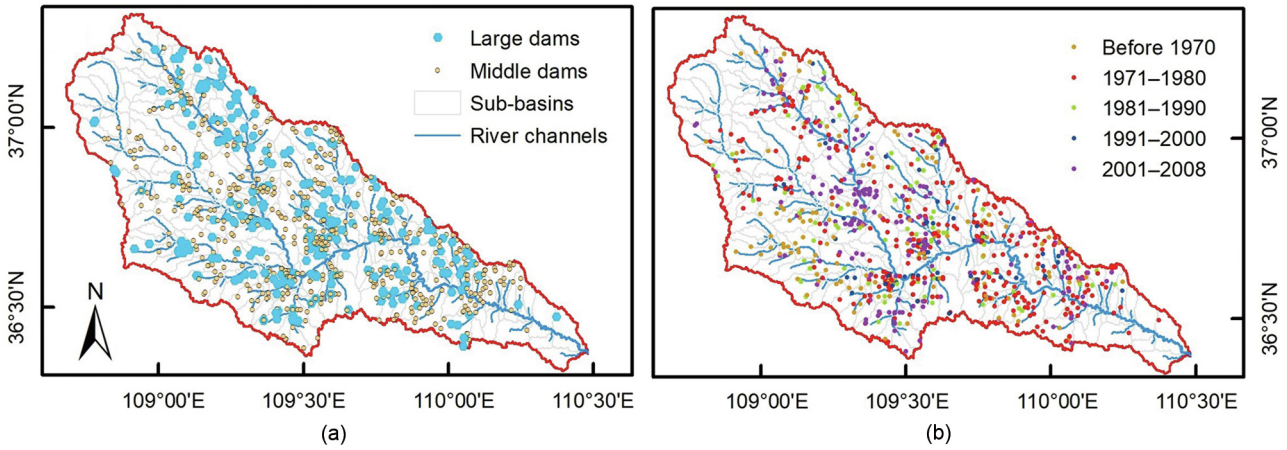

Fig. 2. Check dams in the Yan River Basin: (a) check dam distribution and (b) the construction history.

radiation was estimated based on the duration of sunshine driving the SWAT. In addition, daily precipitation data for three precipitation stations, Ganguyi, Xinshihe and Qingyangcha, were collected from the Hydrological Yearbook of China. Topographic data, a digital elevation model with a resolution of 30 m, were provided by the National Geomatics Center of China[†]. The soil map (1:100 000 scale) was obtained from the National Earth System Science Data Center[‡]. The baseline land use data in 1975 (30 m × 30 m) were also obtained from the National Earth System Science Data Center, representing the land use conditions from 1957 to 1985. Land use maps for 1990, 2000, and 2010, with a resolution of 30 m, obtained from the Institute of Remote Sensing and Digital Earth, Chinese Academy of Sciences, were used to represent the land use conditions during the periods of 1986–1995, 1996–2005, and 2006–2016. The land was divided into six main land use types: grassland, forestland, cropland, water, residential land, and barren land. Hydrological observations used for model calibration and validation were obtained from the Yellow River Conservancy Commission, covering the period of 1957–1970. In addition, a field investigation of check dams in the YanRB was conducted by the Water Department of Shaanxi Province, with a project supervised by the Ministry of Water Resources of the People's Republic of China, providing the survey data for check dams, including their position, construction year, dam height, controlled area, designed storage, and filled storage. Based on the national standard for designed storage [40], check dams were categorized into large (over 5×10^5 m^3), medium (between 5×10^5 and 1×10^5 m^3), and small dams (between 1×10^5 and 1×10^4 m^3). In the

[†] http://www.ngcc.cn/ngcc/
[‡] http://loess.geodata.cn/data/

survey, only large and medium dams were investigated because most of the small dams were constructed by local farmers. Thus, the detailed information on these small dams was not available.

2.4. Dynamic check-dam (DCDam) module

2.4.1. Identification of check dams

As shown in Fig. 2, hundreds of check dams have been implemented in the YanRB, and the connections between them are complete. We divided all the check dams into independent clusters based on the delineated sub-basins provided by the SWAT model. We considered nine check dams in sub-basin 143 as an example (Fig. 3). In this study, we defined all the check dams directly connected to the outlet as first-class check dams. The identification number (ID) of all nine check dams was determined by performing following three steps: ① identify all the first-class check dams (that is, check dams 6, 7, and 9 in Fig. 3(a)), and define their IDs by pasting the dam number to the sub-basin number (that is, 14301, 14302, and 14303 in Fig. 3(b)); ② define all the check dams directly connected to the first-class check dams (e.g., dams 2, 3, and 5 connected to dam 14302) as the second-class dams, and assign them IDs by pasting the dam number to the first-class dam number (e.g., 1430101, 1430102, and 1430103); and ③ assign IDs for all the other check dams following the rules defined in Step 2. Finally, all nine check dams in sub-basin 143 were divided into three classes, and their IDs are displayed in Fig. 3(b). Check dams with higher classes are situated in the upper stream of those with lower classes, and the streamflow and sediment route move from high-class dams to low-class dams in a check dam network.

2.4.2. DCDam module

Fig. 4 illustrates the conceptual scheme that outlines the sediment routing in a check dam network. At a specific time, t, the module identifies all the available check dams based on their construction year and tracks the available storage. Further, it generates a new check dam network with different classes to connect all the available dams at this time point using the ID described in Section 2.4.1. Dams that are not implemented or are already filled completely are defined as unavailable and, thus, cannot be incorporated into a new network. Consequently, a new check dam network is generated for each sub-basin at each time step, and all the check dams in this network can be labeled as class 1 to class n in a sub-basin.

The dynamic storage of a single check dam is calculated based on the sediment balance equations:

$$V_{D,t} = V_{D,t-1} - V_{St,t} \tag{1}$$

$$V_{St,t} = V_{Si,t} - V_{So,t} \tag{2}$$

where $V_{D,t}$ is the available storage at the end of time t, $V_{St,t}$ is the sediment trapped by the check dam at time t, $V_{Si,t}$ is the volume of sediment entering the check dam at time t, and $V_{So,t}$ is the volume of sediment released from the check dam at time t.

As soon as a new network is defined by the dynamic network sub-module (Fig. 4), all the directly connected dams of a specific dam, either upstream or downstream, can be identified, and the $V_{D,t}$ of the highest-class dams can be calculated based on the aforementioned sediment balance equations (Eqs. (1)–(2)). In this study, we assumed that check dams can store all the runoff received from the upper catchment and trap the sediment if the incoming runoff ($V_{Ri,t}$) is less than or equal to the available storage, as mathematically expressed in the following equations:

$$V_{Rs,t} = V_{Ri,t} \tag{3}$$

$$V_{Si,t} = V_{Rs,t} \times C_{con,t} \tag{4}$$

$$V_{Ro,t} = 0 \tag{5}$$

where $V_{Rs,t}$ is the stored runoff at time t, $C_{con,t}$ is the sediment concentration of runoff from the corresponding sub-basin at time t, and $V_{Ro,t}$ is the volume of the released runoff at time t.

Accordingly, if the incoming runoff is larger than the available storage, the amount of runoff exceeding the available storage ($V_{Ro,t}$) and the corresponding sediment is released, and the volume of runoff stored by the check dam equals the available storage, as expressed by the following equations:

$$V_{Rs,t} = V_{D,t-1} \tag{6}$$

$$V_{Ro,t} = V_{Ri,t} - V_{D,t-1} \tag{7}$$

$$V_{So,t} = V_{Ro,t} \times C_{con,t} \tag{8}$$

The incoming runoff can be calculated based on the runoff depth derived from hydrological models, expressed as

$$V_{Ri,t} = A_{a,t} \times H_t \tag{9}$$

where $A_{a,t}$ is the controlled area of the specific check dam at the end of time t, and H_t is the runoff depth of the corresponding sub-basin at time t.

As shown in Fig. 3, several check dams connected with stream channels constitute a dam network. Sediment routes move from

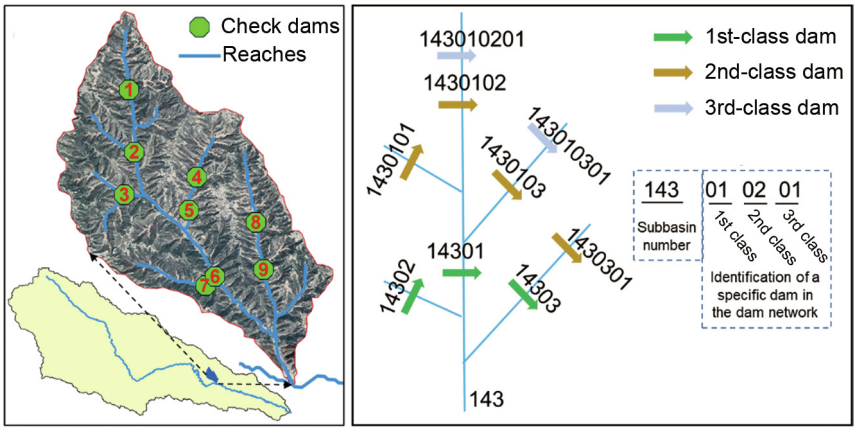

Fig. 3. Identification and Conceptualization of check-dam network in a typical sub-basin: (a) spatial distribution of check dams and (b) the conceptual diagram of the check-dam network.

high-class to low-class dams in a check dam network. Thus, for check dams with the highest class, the actually controlled area ($A_{a,t}$) equals the designed controlled area (A_d). For downstream check dams (check dams with upper dams), runoff and sediment load are first intercepted by the upper check dams implemented in channels, and the actually controlled area ($A_{a,t}$) of the downstream check dams at time t can be described as

$$A_{a,t} = A_d - \sum_{j=1}^{j=m} A_{d,j} \quad (10)$$

where $A_{a,t}$ is the actually controlled area of one specific check dam, A_d is the designed controlled area of the check dam, $A_{d,j}$ is the designed controlled area of directly connected upper check dam j, and m is the number of directly connected upper-stream check dams.

The downstream check dam receives runoff from both its actually controlled area and runoff released from the directly connected upper dams. Thus, the $V_{Ri,t}$ for a downstream dam can be calculated as

$$V_{Ri,t} = V_{Ri,t} + \sum_{j=1}^{j=m} V_{Ro,j,t} \quad (11)$$

where $V_{Ri,t}$ is the volume of runoff generated from the actually controlled area during time t, and $V_{Ro,j,t}$ is the runoff released from one directly connected upper check dam j at time t.

After the calculation for all the check dams at a specific time (time step), the available storage of each check dam is updated, and the module moves to the next time point, $t + 1$, until the completion of the entire study period.

2.4.3. Integration of DCDam and SWAT

The check dams can be simulated using the fully distributed strategy, assigning HRUs for each check dam. This method is employed to re-extract the drainage systems, define the HRUs, and generate the dynamic check dam networks at each time step; thus, the simulation of more than 800 check dams at the watershed scale is challenging. We designed a semi-distributed strategy by assigning a dynamic check dam network for each sub-basin, assuming the same runoff generation and soil erosion intensity for each check dam in a specific sub-basin. In this semi-distributed strategy, we adopted the simulated runoff depth (H_t) and sediment yield ($C_{con,t}$) for each sub-basin from SWAT as inputs to drive the DCDam module (Fig. 5) at each time step.

Finally, the dynamic sediment deposition and sediment released from each check dam were simulated based on the inte-

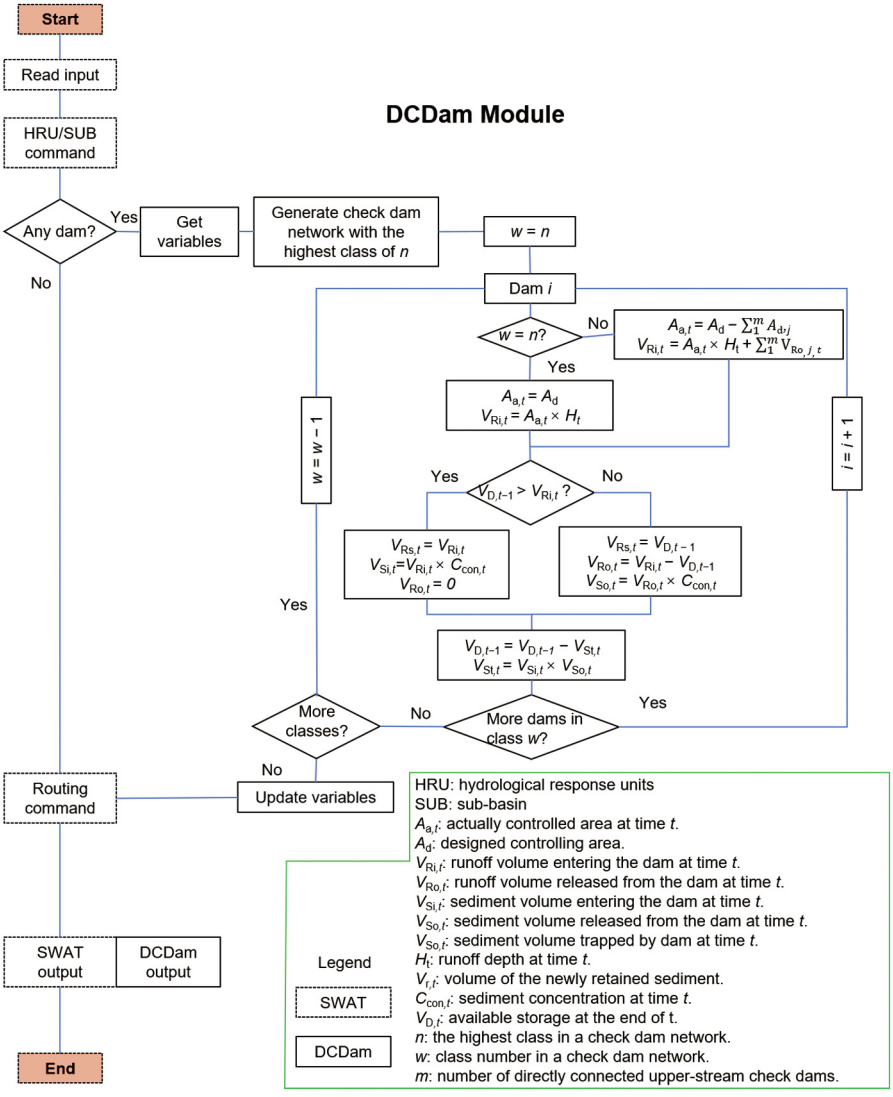

Fig. 4. Operational flowchart of sediment routing in the check-dam network.

gration of SWAT and DCDam modeling, and the outputs were saved in an express sheet for easy post-processing using a common software. The operating procedures and module availability of the SWAT-DCDam framework are presented in Section S1 in Appendix A.

2.5. SWAT model setup and calibration/validation

In this study, the YanRB was subdivided into 202 sub-basins with an average size of 38.25 km^2, and 6053 HRUs were characterized based on the combination of land use, soil, and slope, with an average size of 1.28 km^2. To avoid the effects of check-dam operation on the hydrological modeling by SWAT, the model was calibrated and validated using streamflow and sediment discharge observations that occurred prior to the large-scale construction of check dams in the YanRB: a seven-year (1957–1963) calibration and a seven-year (1964–1970) validation. Based on previous studies and our experiences with SWAT modeling in this region [36,41–43], 13 parameters were selected for streamflow calibration, and three other parameters were selected for sediment (Table 1). Widely accepted statistical metrics were adopted to assess the model performance: the coefficient of determination (R^2), Nash–Sutcliffe efficiency coefficient (NSE), and percent bias (Pbias). Details of the statistical indexes

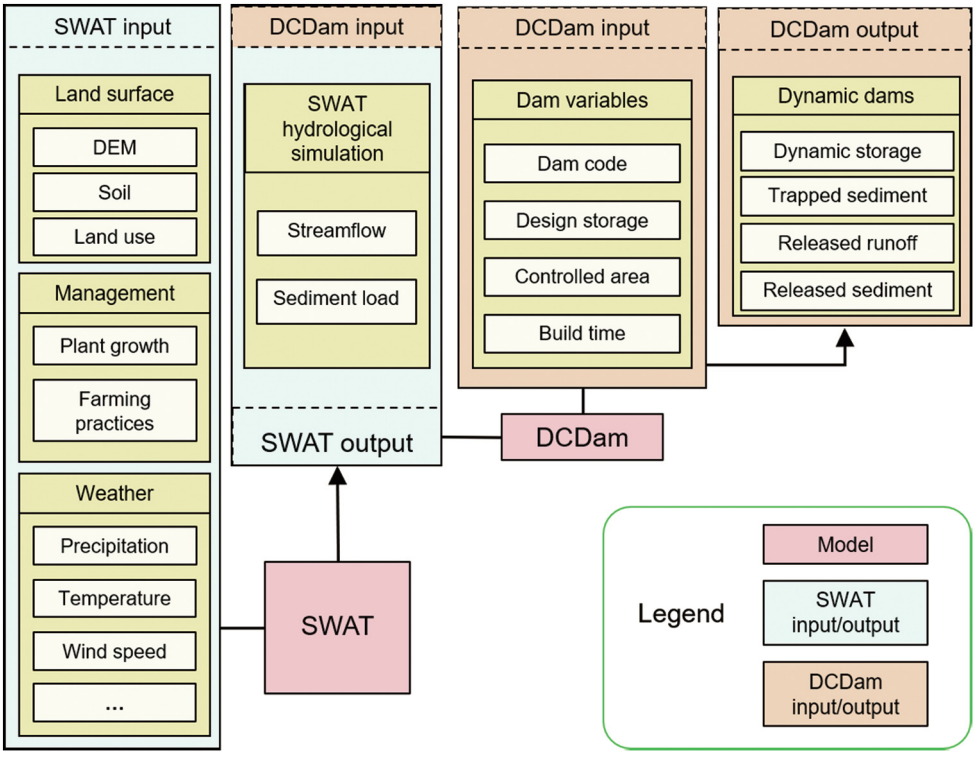

Fig. 5. Framework for integrating the Soil and Water Assessment Tool (SWAT) and Dynamic Check Dam module (DCDam). DEM: digital elevation model.

Table 1
Calibrated SWAT parameters for the YanRB.

Parameter	Definition	Range	Fitted value
CN2	Soil conservation service (SCS) curve number for moisture condition	−10%–10%r	5.3%
SOL_K	Soil saturated hydraulic conductivity (mm·h^{-1})	−10%–10%r	5.2%
SOL_AWC	Soil available water capacity	−10%–10%r	2.9%
SLSUBBSN	Average slope length (m)	35–50v	33.97
HRU_SLP	Average slope steepness (m·m^{-1})	−1035–50v %–10%r	−1.6%
SOL_BD	Bulk density (Mg·m^{-3})	−10%–10%r	−2.7%
ESCO	Soil evaporation compensation coefficient	0.2–0.8v	0.366
SFTMP	Mean air temperature at which precipitation is equally likely to be snow/freezing rain (°C)	0–20v	19.619
SMTMP	Threshold temperature for snowmelt (°C)	0–20v	13.528
SMFMX	Melt factor on December 21 (mm H_2O/day-°C)	0–5v	1.233
USLE_C	Minimum value of the universal soil loss equation (USLE) land cover factor applicable to the land cover/plants	0–0.5v	0.48/0.03/0.001 for cropland/grassland/forestland
USLE_K	Soil erodibility factor (0.013 t·m^2·hr·m^{-3}·MJ^{-1}·cm^{-1})	−10%–10%r	−4.9%
USLE_P	USLE equation support parameter	0–1v	1
CH_K2	Effective hydraulic conductivity of channel (mm·h^{-1})	0–5v	2.3
CANMX	Maximum canopy storage (mm)	0–5v	0.65/2/5 for cropland/grassland/forestland
ALPHA_BF	Baseflow recession constant	0–0.1v	0.015

v means that the existing parameter value is to be replaced by the given value, and r means that the existing parameter value is multiplied by (1 + a given value).

used for model validation are presented in Section S2 in Appendix A.

3. Results

3.1. Check-dam characteristics in the YanRB

The construction history of the check dams in the YanRB is illustrated in Fig. 6. We observe that most of the check dams were constructed in the 1970s, and there were more than 800 check dams by the end of 2008. The construction of check dams was slow during the 1950s and 1960s, with only 63 check dams at the end of 1969, accounting for less than 10% of the total. The construction of check dams in this region was mainly initiated by government-dominant ecological restoration projects, resulting in a boost in check dam construction during the 1970s and 2000s. For example, great enthusiasm was shown in building new check dams in the 1970s because they can help increase food production by cultivating highly productive farmland formed by check dams [44], with more than 300 new dams being constructed in YanRB during this period. Moreover, the dam construction project in the YanRB was evaluated as featured projects by the Ministry of Water Resources of China in 2003, resulting in a boost in dam construction in the 2000s [33]. Both the total controlled area and total storage of check dams increased with the construction of these check dams. By 2008, more than 40% of the basin area was regulated by check dams constructed in channels or gullies. The total storage of check dams in the YanRB reached 350 billion m^3 by the end of 2008, bringing great sediment trapping potential in this region. Check dams can exert immediate and substantial effects on sediment trapping, and intensive check dam building in the 1970s has greatly contributed to sediment load reduction in the YanRB during that period and the subsequent 1980s [45].

The spatial distributions of the large and medium dams are shown in Fig. 2(a); both large and medium dams are distributed uniformly throughout the YanRB. The median storage of large dams is 7.01×10^5 m^3, and that of medium dams is 2.55×10^5 m^3. However, dams built in different time periods may be considerably different, and the key structural parameters may have evolved over time during the past six decades. As illustrated in Fig. 7, the controlled areas of both large and medium dams decrease gradually from the 1960s to 2000s. The median controlled

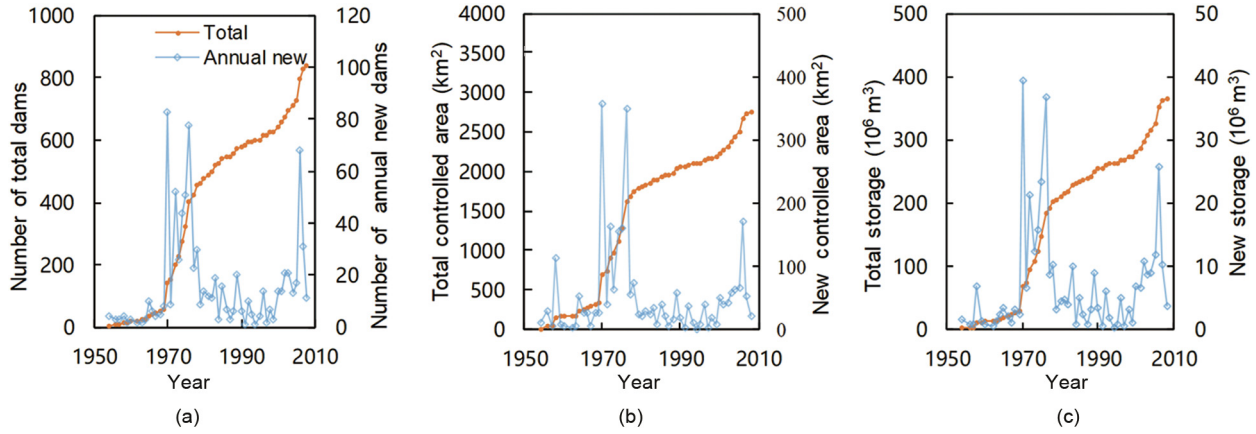

Fig. 6. (a) Number, (b) controlled drainage area, and (c) storage of check dams constructed over the past 60 years in the YanRB.

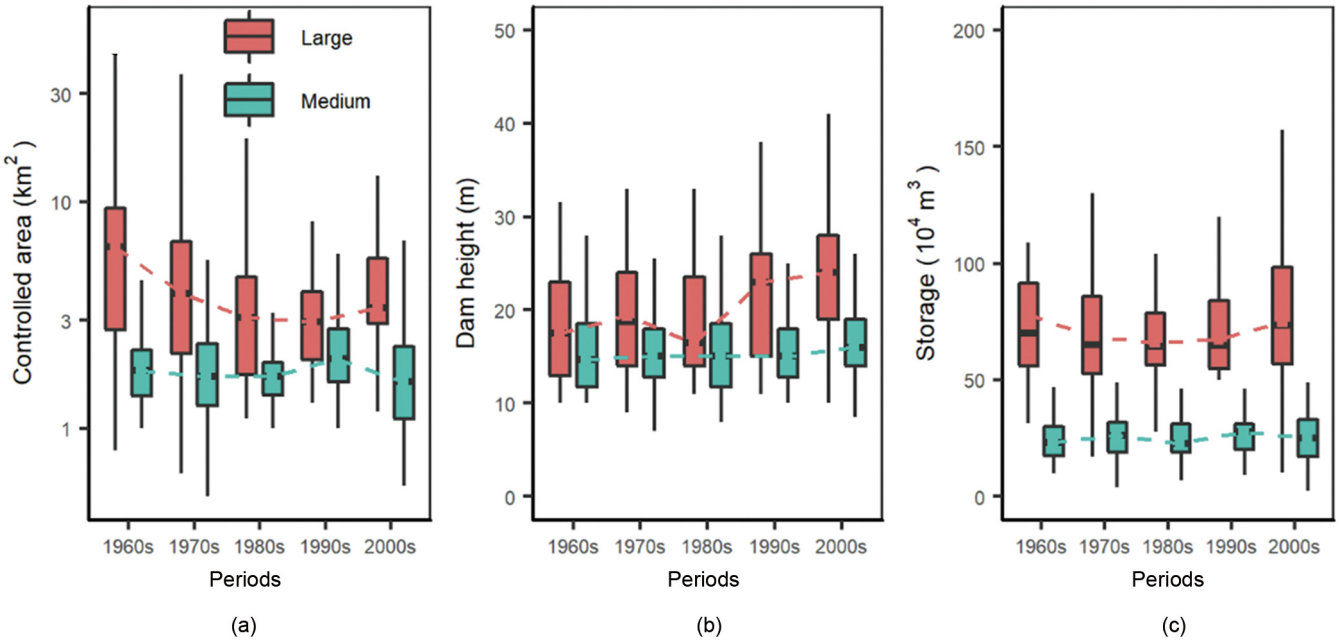

Fig. 7. Designed characteristic parameters of check dams in different time periods: (a) controlled drainage area, (b) dam height, and (c) initial storage.

area for large dams decreased from 6.30 to 3.40 km^2 (46.03% reduction), and that for medium dams decreased from 1.80 to 1.61 km^2 (10.56% decrease). Furthermore, the dam height has increased slowly over the past 60 years. The median height of large dams increased from 17.50 to 24.00 m (37.14% increase), and that for medium dams increased from 14.65 to 16.00 m (9.22% increase). The designed storage is also a vital structural parameter, but there has been no significant trend in the designed storage for the past 60 years. Overall, check dams in the YanRB tend to be higher but have a smaller controlled area. Thus, newly constructed dams seem to be safer because less runoff will be collected from the upper catchment with a decreasing controlled area.

3.2. Performances of the SWAT model and SWAT-DCDam framework

The SWAT model has proven to be useful for simulating sediment yield on the Loess Plateau. In our study, SWAT was calibrated and validated using streamflow and sediment load data observed before the intensive construction of check dams (i.e., 1970s). Fig. 8 illustrates a graphical comparison of simulated streamflow and sediment load against the observations during the seven-year calibration (1957–1963) and seven-year validation (1964–1970) periods. From this figure, the simulated streamflow could capture the variation pattern of observations well. Overall, the streamflow simulation can be rated as "good," with |Pbias| $\leq$ 11%, $R^2 \geq 0.83$, and NSE $\geq$ 0.79 (Table 2) using the widely used criteria proposed by Moriasi et al. [46]. The sediment yield evaluation results revealed that the simulated sediment yield also matched well with the observations, with a 15.4% overestimation and a 14.5% underestimation in the calibration and validation periods, respectively. The simulation of sediment load can be rated as "good," with |Pbias| $\leq$ 15.4%, $R^2 \geq 0.80$, and NSE $\geq$ 0.79 (Table 2). As shown in Fig. S1 in Appendix A, both the simulated annual streamflow and sediment yield matched the observed values well during the entire modeling 60 simulation years (1957–2016), in spite of some overestimations after 2000. In summary, SWAT

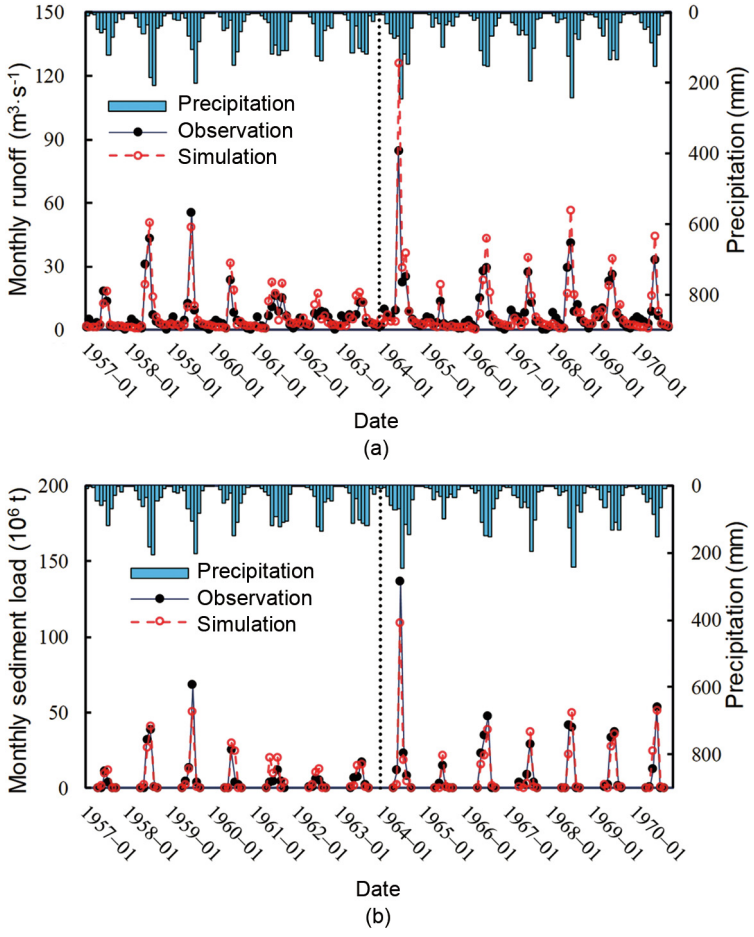

Fig. 8. Monthly comparison of SWAT-simulated versus observed (a) streamflow and (b) sediment during the seven-year calibration (1957–1963) and seven-year validation (1964–1970) periods.

Table 2
Model performance for streamflow and sediment load simulations.

Index	Calibration (1957–1963)		Validation (1964–1970)	
	Runoff	Sediment load	Runoff	Sediment load
R^2	0.83	0.80	0.92	0.93
NSE	0.81	0.79	0.71	0.92
Pbias (%)	7.70	15.40	11.00	−14.50

performed well in both streamflow and sediment simulations and supported the investigation in this study.

Dynamic sediment deposition data are very important; however, they are not directly available. Nonetheless, an investigation on check dams was conducted by the local government at the end of 2008, and the accumulated sediment deposition for each dam was measured. Thus, we validated the SWAT-DCDam framework by comparing the simulated accumulated sediment deposition with the observations from this investigation, as displayed in the scatter plot in Fig. 9. The upper and lower error lines, which indicate the error bounds, were derived by adding or subtracting the percentage of error from the simulated values. The mean values of the observed and simulated accumulated sediment deposition were 2.40×10^5 and 2.68×10^5 m^3, respectively, with an overall overestimation of 11.5%. As shown in Fig. 9, there are some outliers beyond the error range, especially for the simulation of medium check dams. Overall, the statistical metrics indicated that the module can be judged as "satisfactory," with the $|Pbias| \leq 11.5\%$, $R^2 \geq 0.71$, and $NSE \geq 0.50$, based on the sediment evaluation criteria by Moriasi et al. [46], indicating the acceptable performance of DCDam in simulating the dynamic sediment deposition by check dams.

3.3. Dynamic sediment deposition and storage of check dams

Fig. 10 shows the simulated soil erosion intensity in the YanRB during the past 60 years, and no significant trend is observed in this region, with a Z-value of −0.35 using the M–K trend test [47,48]. The mean annual soil erosion intensity is 101.39 $t \cdot ha^{-1} \cdot a^{-1}$, making the YanRB one of the most severe soil erosion regions on the Loess Plateau. As illustrated in Fig. 10(a), the annual amount of sediment trapped by check dams exhibits a significant increasing trend ($p < 0.05$), with a Z-value of 2.26 using the M–K trend test, although it was not monotonous. The amount of sediment trapped by check dams increased moderately for approximately 15 years since the 1950s, increased substantially since 1970, and reached its peak value in 1977; further, the amount of trapped sediment decreased slowly until 2016, except for the extremely high value in 2013 with a record high precipitation.

The construction of new check dams could increase the total available storage, and continuous sediment deposition could fill check dams and decrease the available storage, resulting in the

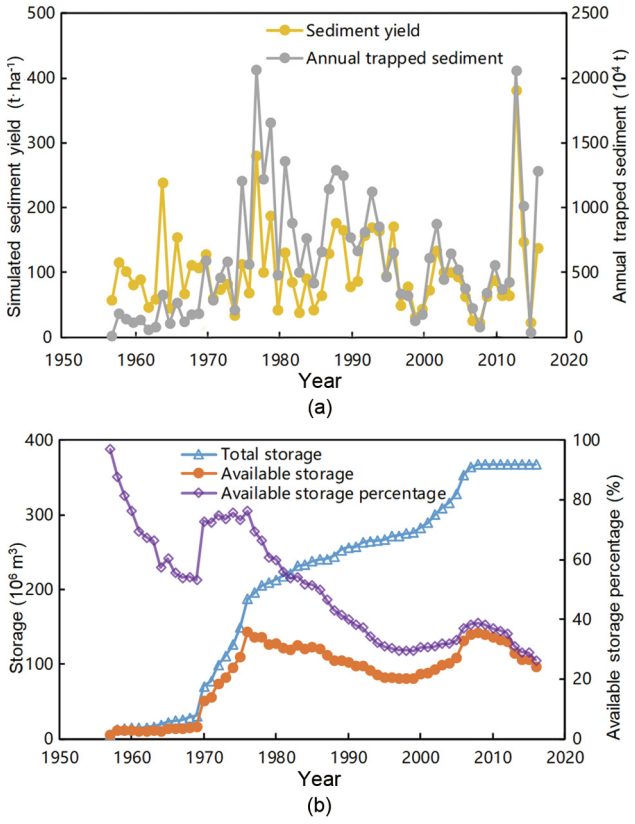

Fig. 10. Amount of (a) sediment yield and sediment trapped by check dams and (b) the dynamic storages of check dams.

complex evolution of the available storage at the watershed scale. As illustrated in Fig. 10(b), the available storage increases rapidly from 1957 to 1977, when the available storage reaches the peak value; this is consistent with the rapid construction of new check dams during this period (Fig. 6). Further, the available storage decreases slowly until 1999; however, the total storage continues to increase. During the 2000s, the construction of new dams increases, resulting in a substantial increase in the available storage. However, the available storage has decreased rapidly in recent years because few new dams have been built since 2008 [33].

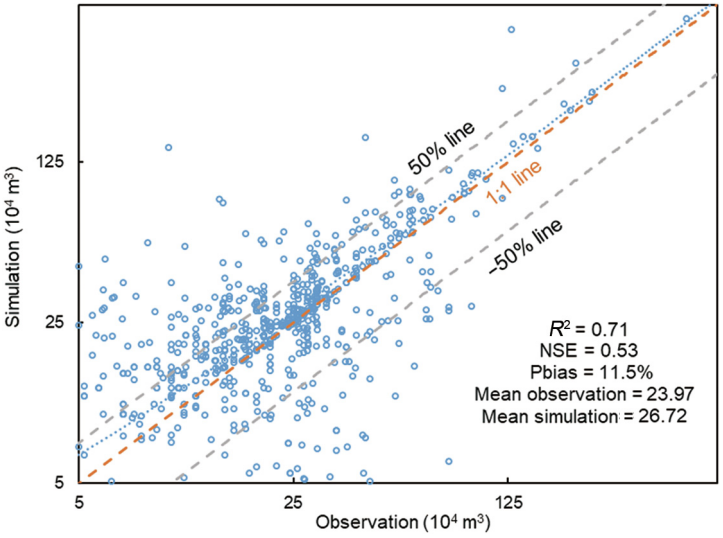

Fig. 9. Scatter plot of simulated and observed accumulated sediment deposition.

Table 3
Contributions of the trapped sediment to sediment load reduction in the Yan River (regions above the Ganguyi (GGY) station).

Period	Sediment load reduction ($\times 10^7$ t)	Sediment retained by check dams ($\times 10^6$ t)	Contributions (%)
1970–1985	2.66	5.84	21.97
1986–1995	1.66	7.27	43.69
1996–2005	3.35	3.68	10.98
2006–2016	5.94	5.02	8.46
1970–2016	3.38	5.07	15.00

3.4. Contributions of sediment trapped by check dams to sediment load reduction in the YanRB

During the past decades, the sediment load in the Yan River has decreased significantly (Fig. S2 in Appendix A), and check dams have played an important role in sediment load reduction in the Yan River. The contributions of the sediment trapped by check dams to sediment load reduction were evaluated by considering the period with few check dams (i.e., from 1957–1969) as the baseline period. As presented in Table 3, the mean annual sediment load reduction is 3.38×10^7 t during 1970–2016 when compared with the baseline sediment load; among this, 5.07×10^6 t of sediment was trapped by check dams, accounting for approximately 15.0% of the total sediment load reduction. The sediment load in rivers was influenced by a few time-varying environmental factors, including climate variation, revegetation, terrace-building, and check-dam construction; thus, sediment load reduction varied considerably during different periods. The mean annual sediment load reduction generally increased from 2.66×10^7 t during 1970–1985 to 5.94×10^7 t during 2006–2016, with relatively low values during 1986–1995. The contributions of the trapped sediment to sediment load reduction first increased from 21.97% (1970–1985) to 43.69% (1986–1995), but then gradually decreased to less than 10% in the last decade (Table 3).

4. Discussion

4.1. Changing environment affected the amount of sediment trapped by check dams

Intensive environmental changes might affect the contributions of trapped sediment to sediment load reduction, complicating the planning and management of check dams. For example, an increase in vegetation cover would decrease the water and sediment supply to check dams [49,50]. Some studies [45,51,52] reported that large-scale greening on the Loess Plateau reduced the sediment yield from slope croplands and altered the following sediment trapping processes before check dams. In the past 40 years, land use patterns in the YanRB have evolved over time, dominated by an increase in forestland and a decrease in cropland, especially since the implementation of the "Grain for Green Project" in the late 1990s (Fig. S3 in Appendix A). In the YanRB, the area of cropland increased slightly from 33.53% in 1975 to 40.20% in 1990 and then decreased to 29.62% in 2000 and further to 17.59% in 2010. Our results revealed that soil erosion changed with the evolution of land use patterns (Fig. S4 in Appendix A). The mean annual sediment load for the four land use scenarios during 1957–2016 was 5.45×10^7, 5.63×10^7, 5.05×10^7, and 3.41×10^7 t, with a 37.43% decrease for the 2010 land use scenario. Fig. 11 presents the mean annual soil erosion intensity during the four time periods (i.e., 1957–1985, 1986–1995, 1996–2005, and 2006–2016 (excluding the extreme wet year, 2013) varying with the combinations of different land use patterns and climate conditions. The mean soil erosion intensity during 2006–2016 is 70.15 $t \cdot ha^{-1}$, approximately 28.29% less than that during 1957–1985.

The annual amount of sediment trapped by check dams was influenced by both the dynamic available storage and soil erosion intensity, which determined the amount of sediment in the check dams, whereas the volume of the trapped sediment was influenced by the available storage. Thus, we listed the trapped sediment and their influencing factors (i.e., soil erosion intensity and available storage) for different time periods in Table 4. The soil erosion intensity during the 1957–1969 period was similar to that in the next period (1970–1985), but the amount of trapped sediment was relatively small because the small available storage limited the sediment trapping of check dams. Further, the combination of large available storage and intensive soil erosion intensity caused a large amount of trapped sediment (more than 8.00×10^6 $t \cdot a^{-1}$) during the 1970–1985 and 1986–1995 time periods. Moreover, the relatively smaller available storage and less intensive soil erosion during 1996–2005 caused less trapped sediment. However, the amount of trapped sediment was much lower, even if the available storage was the largest in the recent period (2006–2016). Thus, we can deduce that the lower soil erosion intensity in the 2010 land use scenario, instead of the available

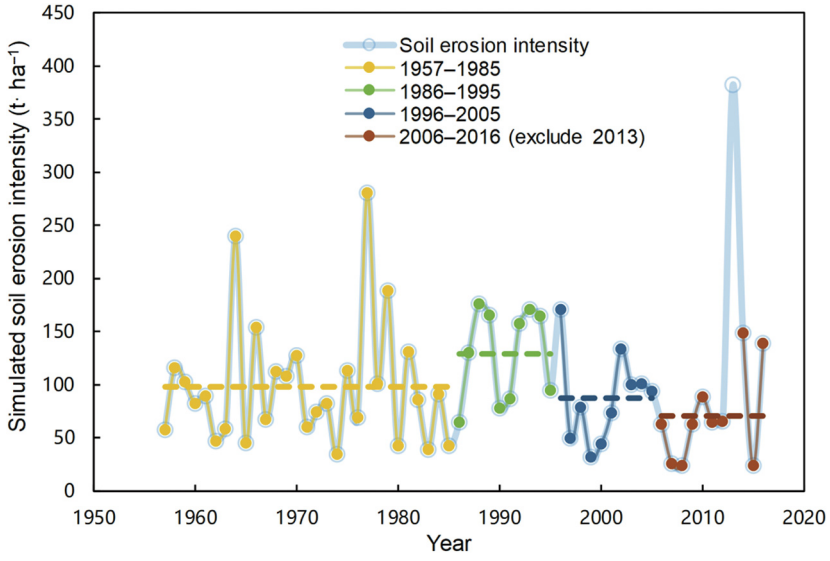

Fig. 11. Simulated soil erosion intensity from 1957 to 2016. The dotted lines are the average value of soil erosion intensity in different time periods.

Table 4
Comparison of the available storage, mean annual soil erosion intensity, and trapped sediment during different time periods.

Period	Available storage ($\times 10^6$ m^3)	Soil erosion intensity (t·ha^{-1}·a^{-1})	Trapped sediment ($\times 10^6$ t·a^{-1})
1957–1969	11.96	98.17	1.48
1970–1985	109.41	97.47	8.30
1986–1995	100.14	128.73	9.04
1996–2005	90.31	87.65	4.72
2006–2016 (exclude 2013)	126.33	70.16	3.57

storage, resulted in a lower level of sediment trapping by check dams. Check dams played a greater role in wet years, with substantially more sediment trapped during those years (Fig. 10(a)). For example, approximately 2.08 $\times$ 10^7 t of sediment were trapped by check dams in 2013, an extreme wet year, accounting for approximately 7.36% of the total sediment yield. Some field investigations have also proven the critical role of check dams during extreme flood events. For example, approximately 40% of the eroded soil (almost 4.89 $\times$ 10^7 t) were reported to have been trapped in check dams during a single extreme flood event in 2017 in the Dali River Basin [53], which is near the YanRB.

4.2. Check-dam planning toward sustainable watershed management

Check-dam construction has been an important ecological restoration measure for sustainable watershed management globally, and it has multiple functions (e.g., water supply enhancement, agricultural land development, and sediment control) [54]. The effects of check dams on supporting sustainable watershed management are becoming more important under changing environments. For example, check dams could decrease the peak runoff discharge and alleviate downstream floods [55]; moreover, intensified droughts due to climate change require the full use of water resources stored in check dams [56]. In the YanRB, more than 3192 hm^2 of plain farmlands had been created by sediment trapped before check dams by the end of 2006 [57], significantly contributing to food security in this region because the productivity of check-dam farmland was approximately 6–10 times higher than that of slope cropland [18]. However, our simulation revealed that more than 75% of dams were approximately full in the YanRB, indicating the potential loss of the effects of check dams and the demand for new check-dam constructions. In addition, our study revealed that more than 40 check dams, approximately 5% of the total check dams, trapped sediment slowly, with less than 30% of the designed storage filled after working for more than 15 years, indicating the necessity and importance of the position chosen for check-dam planning and construction in a watershed. The comprehensive management of check dams requires the prediction of the dynamic storage of check dams. The SWAT-DCDam framework could be a promising tool for simulating the hydrological processes and dynamics of the storage of check dams in a changing environment. Thus, the framework developed in this study can be applied to evaluate the multiple functions of check dams and support the scientific planning and management of new check dams. In addition, this framework can be further developed to extend its functions, such as ecosystem services, a potentially good subject for future studies.

4.3. Limitations and future research

Model integration is a promising method for investigating complex environmental challenges [58]. In this study, the newly developed DCDam module was integrated with the widely used SWAT model to simulate the dynamic sediment trapping by check dams at the watershed scale. However, the SWAT-DCDam was subject to various uncertainties, including modeling and data uncertainties, as more processes were included when integrating both models [59].

The model structures for both SWAT and DCDam were not perfect and could be improved in the future, especially when considering the changing land surface conditions caused by intense environmental changes. For most hydrological models, the real hydrological processes are depicted by functions and parameters, and these parameters are calibrated to minimize model biases [60]. The effects of land use change are simulated by utilizing time-varying land use inputs, but constant optimal model parameters for the same land use type. However, hydrological processes might change after intense land use change. For example, the runoff generation mechanism might have changed after the extensive revegetation on the Loess Plateau [61], and the percentage of Hortonian overland flow has been decreasing [62]. Thus, the model structures can be improved further to better describe the hydrological processes in regions with extensive human disturbances.

The complex operating systems made it difficult to fully describe the operational effects of check dams on runoff and sediment processes. On the one hand, runoff exceeding the available storage would be spilled over dam embankment or through spillways. On the other hand, clean water after sediment deposition would be drained out through the tunnels. In this study, we assumed that the sediment concentration for the spilled runoff was the same as that for the incoming runoff. However, the sediment concentration might be smaller than the incoming runoff because the flood velocity and sediment concentration for runoff flow through the deposition area would significantly decrease [63]. For large reservoirs, Brune [64] collected the operation data and proposed a function by correlating the trapping capacity with the available storage–inflow ratio, which is widely used globally. However, more than 60% of the sediment was trapped even though the available storage–inflow ratio was smaller than 0.01 (much higher for check dams on the Loess Plateau), based on the sediment regulation function proposed by Brune (Fig. S5 in Appendix A). Our hypothesis (sediment in the released runoff was the same as that for inflow) in this study might underestimate the percentage of sediment deposited before check dams. Thus, more field investigations (e.g., the sediment trapping efficiency for check dams with different available storages) should be performed to better conceptualize sediment deposition and drainage processes, particularly the sediment trapping ratio. In this study, the DCDam module was integrated into the SWAT model using a semi-distributed strategy, by assuming that the runoff generation and sediment yield intensity were homogeneous for a specific sub-basin, and uncertainties were introduced by ignoring the spatial heterogeneity of runoff generation and sediment yield.

The availability and reliability of data, especially field measurement data, could cause large uncertainties in the use of the SWAT-DCDam framework, and there may be limitations in the study. Numerous small check dams were constructed by local farmers from 1950 to 1980 [65], and these dams were mostly filled when the investigation was conducted in 2009. Thus, the small dams were not included in this study. Moreover, the total deposited sediment before check dams was measured by different teams using different surveying methods, indicating potential uncertainties for the validation results in this study. Furthermore, some crucial structural parameters of check dams (e.g., the size and position of the spillways and tunnels) were not surveyed in this investigation, limiting the improvements of the DCDam module. New technologies would be valuable in obtaining more information for further improvements of DCDam. For example, remote sensing technologies, especially the widely used unmanned aerial systems,

can be used to detect the positions and controlled areas of check dams, as well as the accumulated deposition storages when combined with the digital elevation models in different periods [66], providing data to improve the conceptualization and validation of the SWAT-DCDam model in the future.

5. Conclusions

In this study, we proposed the SWAT-DCDam framework for modeling the dynamic sediment trapped in check dam networks, by integrating a newly developed module, DCDam, and the widely used watershed hydrological model (SWAT). This framework was tested and applied by conducting a case study of a typical Loess watershed in the Yellow River Basin, the YanRB. Our evaluation results revealed that the developed SWAT-DCDam can simulate the available check-dam storage and sediment trapped by check dams dynamically in the check dam networks in a watershed. As indicated in the case study of the YanRB, the designed structure of check dams has evolved over the past 60 years, with higher dams but less controlled areas in recent years. Check dams have been an important soil conservation measure in the YanRB, contributing 15.0% of the sediment load reduction in the Yan River. However, the contribution of the trapped sediment to sediment load reduction has decreased, and the contribution of check dams has decreased to approximately 10% in the last decade. Moreover, our simulation results revealed that more than 75% of check dams in the YanRB are almost full, indicating a potential demand for the construction of new check dams in this watershed. Overall, the developed SWAT-DCDam framework could be a promising tool for investigating the dynamic sediment trapping in check-dam networks in a changing environment. The assessment results of the check-dam networks in the YanRB could provide useful information to support decision-making when planning and constructing a check dam for sustainable watershed management.

Acknowledgments

This study was funded by the Strategic Priority Research Program of Chinese Academy of Sciences (XDB40020205), the National Natural Science Foundation of China (U2243210, 42041006, and 31961143011), Key laboratory of Degraded and Unused Land Consolidation Engineering of Natural Resources Ministry of China (SXDJ2019-5), the Key Research and Development Program of Shaanxi Province (2022ZDLSF06-04), the Innovation Team of Shaanxi Province (2021TD-52), the Key Laboratory of Eco-Environment and Meteorology for the Qinling Mountains and Loess Plateau, Shaanxi Meteorological Bureau (2021K-6), the Technology Innovation Center for Land Engineering and Human Settlements, Shaanxi Land Engineering Construction Group Co., Ltd. and Xi'an Jiaotong University (201912131-B2), the "Light of the West" talent program of the Chinese Academy of Science, the Key Research and Development Project in Shaanxi Province (S2020-YF-GHZD-0061), the National Thousand Youth Talent Program of China, and the Shaanxi Hundred Talent Program. We thank the High Performance Computing Cluster (HPCC) Platform in Xi'an Jiaotong University for computing equipment and computer maintenance. We also thank the editor and five anonymous reviewers for their constructive comments and suggestions.

Appendix A. Supplementary data

Supplementary data to this article can be found online at https://doi.org/10.1016/j.eng.2021.12.015.

References

[1] Borrelli P, Robinson DA, Fleischer LR, Lugato E, Ballabio C, Alewell C, et al. An assessment of the global impact of 21st century land use change on soil erosion. Nat Commun 2017;8:2013.
[2] Lal R. Soil erosion impact on agronomic productivity and environment quality. Crit Rev Plant Sci 1998;17(4):319–464.
[3] Panagos P, Katsoyiannis A. Soil erosion modelling: the new challenges as the result of policy developments in Europe. Environ Res 2019;172:470–4.
[4] Keesstra SD, Bouma J, Wallinga J, Tittonell P, Smith P, Cerdà A, et al. The significance of soils and soil science towards realization of the United Nations Sustainable Development Goals. Soil (Gottingen) 2016;2(2):111–28.
[5] Visser S, Keesstra S, Maas G, De Cleen M, Molenaar C. Soil as a basis to create enabling conditions for transitions towards sustainable land management as a key to achieve the SDGs by 2030. Sustainability 2019;11(23):6792.
[6] Abbasi NA, Xu X, Lucas-Borja ME, Dang W, Liu B. The use of check dams in watershed management projects: examples from around the world. Sci Total Environ 2019;676:683–91.
[7] Lucas-Borja ME, Piton G, Nichols M, Castillo C, Yang Y, Zema DA. The use of check dams for soil restoration at watershed level: a century of history and perspectives. Sci Total Environ 2019;692:37–8.
[8] Piton G, Carladous S, Recking A, Tacnet JM, Liébault F, Kuss D, et al. Why do we build check dams in Alpine streams? An historical perspective from the French experience. Earth Surf Process Landf 2017;42(1):91–108.
[9] Robichaud PR, Storrar KA, Wagenbrenner JW. Effectiveness of straw bale check dams at reducing post-fire sediment yields from steep ephemeral channels. Sci Total Environ 2019;676:721–31.
[10] Galicia S, Navarro-Hevia J, Martínez-Rodríguez A, Mongil-Manso J, Santibáñez J. 'Green', rammed earth check dams: a proposal to restore gullies under low rainfall erosivity and runoff conditions. Sci Total Environ 2019;676:584–94.
[11] Alfonso-Torreño A, Gómez-Gutiérrez Á, Schnabel S, Lavado Contador JF, de Sanjosé Blasco JJ, Sánchez Fernández M. sUAS, SfM-MVS photogrammetry and a topographic algorithm method to quantify the volume of sediments retained in check-dams. Sci Total Environ 2019;678:369–82.
[12] Ministry of Water Resources of China.. Bulletin of first national water census for soil and water conservation. Beijing: China Water Power Press; 2013.
[13] Zhao G, Kondolf GM, Mu X, Han M, He Z, Rubin Z, et al. Sediment yield reduction associated with land use changes and check dams in a catchment of the Loess Plateau, China. Catena 2017;148:126–37.
[14] Bai L, Wang N, Jiao J, Chen Y, Tang B, Wang H, et al. Soil erosion and sediment interception by check dams in a watershed for an extreme rainstorm on the Loess Plateau. China Int J Sediment Res 2020;35(4):408–16.
[15] Liu Y, Liu Y, Shi Z, López-Vicente M, Wu G. Effectiveness of re-vegetated forest and grassland on soil erosion control in the semi-arid Loess Plateau. Catena 2020;195:104787.
[16] Yuan S, Li Z, Li P, Xu G, Gao H, Xiao L, et al. Influence of check dams on flood and erosion dynamic processes of a small watershed in the Loss Plateau. Water 2019;11(4):834.
[17] Conesa-García C, López-Bermúdez F, García-Lorenzo R. Bed stability variations after check dam construction in torrential channels (South-East Spain). Earth Surf Process Landf 2007;32(14):2165–84.
[18] Wang Y, Fu B, Chen L, Lü Y, Gao Y. Check dam in the Loess Plateau of China: engineering for environmental services and food security. Environ Sci Technol 2011;45(24):10298–9.
[19] Mongil-Manso J, Díaz-Gutiérrez V, Navarro-Hevia J, Espina M, San Segundo L. The role of check dams in retaining organic carbon and nutrients. A study case in the Sierra de Ávila mountain range (Central Spain). Sci Total Environ 2019;657:1030–40.
[20] Keesstra S, Nunes JP, Saco P, Parsons T, Poeppl R, Masselink R, et al. The way forward: can connectivity be useful to design better measuring and modelling schemes for water and sediment dynamics? Sci Total Environ 2018;644:1557–72.
[21] Vaezi AR, Abbasi M, Keesstra S, Cerdà A. Assessment of soil particle erodibility and sediment trapping using check dams in small semi-arid catchments. Catena 2017;157:227–40.
[22] Zhao G, Mu X, Han M, An Z, Gao P, Sun W, et al. Sediment yield and sources in dam-controlled watersheds on the northern Loess Plateau. Catena 2017;149:110–9.
[23] Chen F, Fang N, Wang Y, Tong L, Shi Z. Biomarkers in sedimentary sequences: indicators to track sediment sources over decadal timescales. Geomorphology 2017;278:1–11.
[24] Abedini M, Md Said MA, Ahmad F. Effectiveness of check dam to control soil erosion in a tropical catchment (The Ulu Kinta Basin). Catena 2012;97:63–70.
[25] Wei Y, He Z, Li Y, Jiao J, Zhao G, Mu X. Sediment yield deduction from check-dams deposition in the weathered sandstone watershed on the North Loess Plateau, China. Land Degrad Dev 2017;28(1):217–31.
[26] Ramos-Diez I, Navarro-Hevia J, San Martín Fernández R, Mongil-Manso J. Final analysis of the accuracy and precision of methods to calculate the sediment retained by check dams. Land Degrad Dev 2017;28(8):2446–56.
[27] Wang X, Jin Z, Zhang X, Xiao J, Zhang F, Pan Y. High-resolution geochemical records of deposition couplets in a palaeolandslide-dammed reservoir on the Chinese Loess Plateau and its implication for rainstorm erosion. J Soils Sed 2018;18:1147–58.

[28] Wei Y, He Z, Jiao J, Li Y, Chen Y, Zhao H. Variation in the sediment deposition behind check-dams under different soil erosion conditions on the Loess Plateau. China Earth Surf Process Landf 2018;43(9):1899–912.
[29] Li E, Mu X, Zhao G, Gao P, Sun W. Effects of check dams on runoff and sediment load in a semi-arid river basin of the Yellow River. Stochastic Environ Res Risk Assess 2017;31(7):1791–803.
[30] Pal D, Galelli S, Tang H, Ran Q. Toward improved design of check dam systems: a case study in the Loess Plateau, China. J Hydrol (Amst) 2018;559:762–73.
[31] Fu B, Wang S, Liu Y, Liu J, Liang W, Miao C. Hydrogeomorphic ecosystem responses to natural and anthropogenic changes in the Loess Plateau of China. Annu Rev Earth Planet Sci 2017;45(1):223–43.
[32] Zhao G, Mu X, Wen Z, Wang F, Gao P. Soil erosion, conservation, and eco-environment changes in the Loess Plateau of China. Land Degrad Dev 2013;24 (5):499–510.
[33] Wei Y. Characteristics of sediment deposition of typical check-dams and its effect on the sediment discharge variation of Yanhe and Huangfuchuan River Basin, in research center of soil and water conservation and ecological environment [dissertation]. Yangling: the University of Chinese Academy of Sciences; 2017. Chinese.
[34] Arnold JG, Srinivasan R, Muttiah RS, Williams JR. Large area hydrologic modeling and assessment part I: model development. J Am Water Resour As 1998;34(1):73–89.
[35] Neitsch SL, Arnold JG, Kiniry JR, Williams JR. Soil and water assessment tool: theoretical documentation. Report. College Station, Texas: Texas A&M University System: College Station, Texas; 2011.
[36] Sun P, Wu Y, Wei X, Sivakumar B, Qiu L, Mu X, et al. Quantifying the contributions of climate variation, land use change, and engineering measures for dramatic reduction in streamflow and sediment in a typical loess watershed, China. Ecol Eng 2020;142:105611.
[37] Zhang X. Simulating eroded soil organic carbon with the SWAT-C model. Environ Model Softw 2018;102:39–48.
[38] Hu J, Wu Y, Wang L, Sun P, Zhao F, Jin Z, et al. Impacts of land-use conversions on the water cycle in a typical watershed in the Southern Chinese Loess Plateau. J Hydrol 2021;593:125741.
[39] Arnold J, Kiniry J, Srinivasan R, Williams J, Haney E, Neitsch S. SWAT 2012 input/output documentation. Report. College Station, Texas: Water Resources Institute; 2013.
[40] Standardization Administration of China (SAC). GB/T 16453.3-2008: comprehensive control of soil and water conservation—technical specification—technique for erosion control of gullies. Chinese standard. Beijing: Standardization Administration of China (SAC); 2008. Chinese.
[41] Wang Y, Fang N, Zhang F, Wang L, Wu G, Yang M. Effects of erosion on the microaggregate organic carbon dynamics in a small catchment of the Loess Plateau, China. Soil Tillage Res 2017;174:205–13.
[42] Zhao F, Wu Y, Qiu L, Sun Y, Sun L, Li Q, et al. Parameter uncertainty analysis of the SWAT model in a mountain-loess transitional watershed on the Chinese Loess Plateau. Water 2018;10(6):690.
[43] Xu Y, Fu B, He C. Assessing the hydrological effect of the check dams in the Loess Plateau, China, by model simulations. Hydrol Earth Syst Sci 2013;17 (6):2185–93.
[44] Xu X, Zhang H, Zhang O. Development of check-dam systems in gullies on the Loess Plateau. China Environ Sci Policy 2004;7(2):79–86.
[45] Sun P, Wu Y, Yang Z, Sivakumar B, Qiu L, Liu S, et al. Can the Grain-for-Green program really ensure a low sediment load on the Chinese Loess Plateau? Engineering 2019;5(5):855–64.
[46] Moriasi DN, Arnold JG, Van Liew MW, Bingner RL, Harmel RD, Veith TL. Model evaluation guidelines for systematic quantification of accuracy in watershed simulations. T ASABE 2007;50(3):885–900.
[47] Mann H. Nonparametric tests against trend. Econometrica 1945;13(3):245–59.
[48] Kendall MG. Rank correlation measures. 4th ed. London, UK: Charles Griffin; 1975.
[49] Lucas-Borja ME, Zema DA, Hinojosa Guzman MD, Yang Yu, Hernández AC, Xiangzhou Xu, et al. Exploring the influence of vegetation cover, sediment storage capacity and channel dimensions on stone check dam conditions and effectiveness in a large regulated river in México. Ecol Eng 2018;122:39–47.
[50] Rodrigo-Comino J, Terol E, Mora G, Giménez-Morera A, Cerdà A. Vicia sativa Roth. can reduce soil and water losses in recently planted vineyards (Vitis vinifera L.). Earth Syst Environ 2020;4(4):827–42.
[51] Wang W, Fang N, Shi Z, Lu X. Prevalent sediment source shift after revegetation in the Loess Plateau of China: implications from sediment fingerprinting in a small catchment. Land Degrad Dev 2018;29 (11):3963–73.
[52] Liang Y, Jiao J. Characteristics of sediment retention by check-dams before and after the “Grain for Green” project in the He-Long Reach of the Yellow River. Acta Ecol Sin 2019;39(12):4579–86.
[53] Yu X, Hou S, Li Y, Shi X. Identifying sediment sources in Wuding River during “7.26” flood in 2017. Hydro-science and Engineering 2019;(06):31–7. Chinese.
[54] Lucas-Borja ME, Piton G, Yu Y, Castillo C, Antonio Zema D. Check dams worldwide: objectives, functions, effectiveness and undesired effects. Catena 2021;204:105390.
[55] Wang T, Hou J, Li P, Zhao J, Li Z, Matta E, et al. Quantitative assessment of check dam system impacts on catchment flood characteristics–a case in hilly and gully area of the Loess Plateau. China Nat Hazards 2021;105(3):3059–77.
[56] Yang J, Shi X, Zuo Z, Kong X, Xiao P. Survey and analysis on the construction and operation of warping dams in He'nan province. Soil Water Conserv 2020;10:10–2. Chinese.
[57] Ran D, Zuo Z, Wu Y, Li XM, Li ZH, et al. Recent changes of streamflow and sediment load in the middle Yellow River Basin and their responses to human activities. Beijing: Science Press; 2012. Chinese.
[58] Wu Y, Liu S, Qiu L, Sun Y. SWAT-DayCent coupler: an integration tool for simultaneous hydro-biogeochemical modeling using SWAT and DayCent. Environ Model Softw 2016;86:81–90.
[59] Sun P, Wu Y, Xiao J, Hui J, Hu J, Zhao F, et al. Remote sensing and modeling fusion for investigating the ecosystem water-carbon coupling processes. Sci Total Environ 2019;697:134064.
[60] Borrelli P, Van Oost K, Meusburger K, Alewell C, Lugato E, Panagos P. A step towards a holistic assessment of soil degradation in Europe: coupling on-site erosion with sediment transfer and carbon fluxes. Environ Res 2018;161:291–8.
[61] Mu X, Gu C, Sun W, Zhao G, Gao P, Wang S. Preliminary assessment effect of vegetation restoration on runoff generation pattern of the Loess Plateau. Yellow River 2019;41(10):33–41. Chinese.
[62] Zhang L, Hu C, Jian S, Wu Q, Ran G, Xu Y. Identifying dominant component of runoff yield processes: a case study in a sub-basin of the middle Yellow River. Hydrol Res 2021;52(5):1033–47.
[63] Ran Q, Tang H, Wang F, Gao J. Numerical modelling shows an old check-dam still attenuates flooding and sediment transport. Earth Surf Proc Land 2021;46 (8):1549–67.
[64] Brune GM. Trap efficiency of reservoirs. Eos (Wash DC) 1953;34(3):407–18.
[65] Liu X, Gao Y, Ma S. Dong GT Sediment reduction of warping dams and its timeliness in the Loess Plateau. J Hydraul Eng 2018;49(02):145–55.
[66] Rodrigues BT, Zema DA, González-Romero J, Rodrigues MT, Campos S, Galletero P, et al. The use of unmanned aerial vehicles (UAVs) for estimating soil volumes retained by check dams after wildfires in mediterranean forests. Soil Syst 2021;5(1):9.